Equivalent Circuits of Junctions of Slab-Loaded Rectangular Waveguides

ALFRED T. VILLENEUVE, SENIOR MEMBER, IEEE

Abstract —**Equivalent-circuit parameters are calculated for junctions of dielectrically loaded rectangular waveguides. The loading takes the form of axial slabs consisting of dielectric sandwich structures. Two different forms of the equivalent circuit are considered. One form, which consists of an ideal transformer between two sections of transmission line, appears to be the most natural for these junctions. A number of examples are given.**

I. Introduction

THE DESIGN OF waveguide systems sometimes demands that waveguides be loaded with longitudinal dielectric slabs in the form of either single dielectrics or sandwich structures. Often, however, the use of such devices creates junctions between guides with different loadings. Consequently, the equivalent-circuit parameters of such junctions should be determined so that their effect on system performance can be predicted. In this paper, the equivalent-circuit elements of several junctions are evaluated for this purpose.

Chang [1], [2] analyzed the junctions of rectangular guides in which each guide had different slab-loading configurations that were asymmetrically arranged about the centerline. Only one dielectric was considered in each guide. For these junctions, Chang computed values of the elements of the equivalent circuit shown in Fig. 1. Chang's approach made use of a moment method in which the scattering matrix and then the elements of the T network were computed, necessitating the solution of two problems: one in which the excitation was incident from the first guide and another in which the excitation was incident from the second guide. The method also required that the propagation constant of each mode used be determined through the solution of a transcendental equation. It then necessitated that the corresponding modal field distributions be ascertained for use in the moment method.

The method used here differs from that of Chang in several important respects. First, the guide loading differs from that considered by Chang in that the dielectric materials can be sandwich-type structures consisting of two dielectrics (Fig. 2). Only symmetrical structures are considered here. Second, two different equivalent-circuit forms are considered (Figs. 3 and 4), which are the same as those used by Collin [3]–[5]. The form in Fig. 4 would appear to be the most natural for the junctions considered here, since the transformer ratio comes out to be very nearly unity in all cases, and one immediately sees that the main effect of the junction is to make the effective lengths of the lines slightly different from their physical lengths. Thus, the primary effect of higher order modes at the junction is to modify the phases—but not the magnitudes—of the transmission and reflection coefficients. This conclusion is not immediately evident from the equivalent circuits of Figs. 1 and 3.

A third distinction between this method and Chang's lies in the fact that the Rayleigh–Ritz method is used in the current approach to determine the mode configurations and propagation constants in the loaded guides; thus, no solutions of transcendental equations are necessary [3]. Further, only a single problem need be solved to obtain the complete equivalent circuit. Finally, the circuit parameters are obtained through the use of a method that does not require a direct solution to the equations expressing continuity of the fields across the junction.

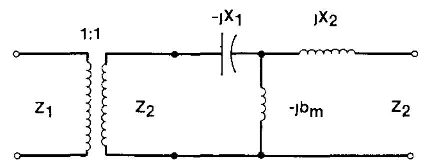

Fig. 1. Chang's equivalent circuit of junction of slab-loaded guides.

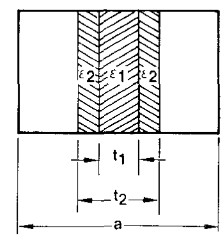

Fig. 2. Sandwich structure of two dielectrics in rectangular waveguide.

Manuscript received June 4, 1984; May 6, 1985.
The author is with the Antenna Systems Laboratory, Radar Systems Group, Hughes Aircraft Company, El Segundo, CA.

0018-9480/85/1100-1196$01.00 ©1985 IEEE

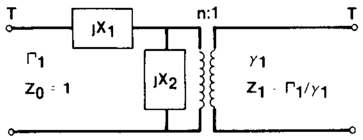

Fig. 3. Collin's lumped-element equivalent circuit.

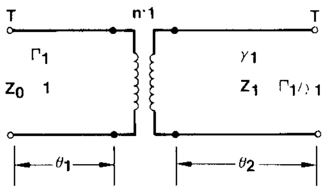

Fig. 4. Collin's transmission-line form of equivalent circuit.

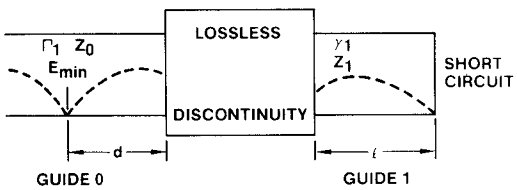

Fig. 5. Lossless discontinuity between two waveguides.

The approach used herein expands the mode functions of the loaded guide in terms of the modes of the empty guide. In this method, the propagation constant and expansion coefficients are determined by means of the Rayleigh–Ritz technique. The mode functions are then used in a field-matching technique across the junction to generate an equation from which the equivalent-circuit parameters can be deduced.

II. Discussion

A. Equivalent-Circuit Forms

The problem to be treated is similar to that described in Collin [3] except that the cross sections of the guide have a different loading configuration. The general configuration to be analyzed is shown in Fig. 5. In this configuration, the short-circuit termination keeps all field quantities real, thereby simplifying numerical computations. The distance d in guide 0 represents the distance from the junction to the position where the electric field of the dominant mode vanishes. It has been shown that $|\Gamma_1|d$ and $|\gamma_1|l$ are related by the following equation [6]:

$$\tan|\Gamma_1|d = \frac{A + B\tan|\gamma_1|l}{C + D\tan|\gamma_1|l} \tag{1}$$

where A, B, C, and D are constants of the particular discontinuity and Γ_1 and γ_1 are the dominant mode propagation constants in guides 0 and 1, respectively.

The elements of the equivalent circuit of Fig. 3 are given in terms of A, B, C, and D as follows [3]:

$$X_1 = -\frac{A}{C} \tag{2a}$$

$$X_2 = \frac{A}{C} - \frac{B}{D} \tag{2b}$$

$$n^2 Z_1 = \frac{DA}{C^2} - \frac{B}{C}. \tag{2c}$$

The elements of the equivalent circuit of Fig. 4 can be shown to be given by the following expressions (see Appendix I):

$$\theta_2 = \frac{1}{2}\left[\tan^{-1}\left(\frac{A+D}{B-C}\right) + \tan^{-1}\left(\frac{A-D}{B+C}\right)\right] \tag{2d}$$

$$\theta_1 = \frac{1}{2}\left[\tan^{-1}\left(\frac{A+D}{B-C}\right) - \tan^{-1}\left(\frac{A-D}{B+C}\right)\right] \tag{2e}$$

$$n^2 Z_1 = \frac{\tan\theta_1 - \frac{A}{D}\tan\theta_2}{\frac{A}{D}\tan\theta_1 - \tan\theta_2}. \tag{2f}$$

The expressions for A, B, C, and D can be found by solving the boundary-value problem for the particular junction of interest. This solution is considered in the sections that follow.

B. Eigenvalues and Eigenfunctions

The eigenvalues and eigenfunctions of the dielectrically loaded waveguides are determined through the use of the Rayleigh–Ritz method as described by Collin [3]. For the geometry under consideration, the modes excited are longitudinal-section E (LSE) modes, which have no component of E normal to the dielectric slab surfaces. In addition, there is no field variation from the top to the bottom of the guide. These modes may be approximated as closely as desired by a linear combination of modes of the empty waveguide. The appropriate empty-waveguide modes are given by

$$f_n(x) = \sqrt{\frac{2}{a}}\sin\left(\frac{n\pi}{a}x\right), \qquad n = 1, 2, \cdots. \tag{3}$$

The eigenfunctions $\phi_m(x)$ of the loaded guide can be approximated as a linear combination of the f_n as follows:

$$\phi_m(x) = \sum_{n=1}^{N} a_n^{(m)} f_n(x). \tag{4}$$

As N increases, the approximation improves.

The eigenfunctions $\phi_m(x)$ are solutions of the following equation:

$$\frac{d^2\phi_m}{dx^2} + \left[\gamma_m^2 + \epsilon_r(x)k_0^2\right]\phi_m(x) = 0 \tag{5}$$

with ϕ_m vanishing at $x = 0$ and $x = a$. From this equation, it is possible to derive the following stationary expression for the γ_m:

$$\gamma_m = \frac{\int_0^a \left[\left(\frac{d\phi_m}{dx} \right)^2 - \epsilon_r k_0^2 \phi_m^2 \right] dx}{\int_0^a \phi_m^2 \, dx}. \tag{6}$$

If (4) is substituted into (6) and the stationary property of (6) is employed, the following system of simultaneous equations is obtained for the $a_n^{(m)}$:

$$\sum_{n=1}^{N} a_n^{(m)} \left(T_{pn} - \gamma_m^2 \delta_{np} \right) = 0, \qquad p = 1, 2, \cdots, N \tag{7}$$

where

$$T_{pn} = T_{np} = \int_0^a \left[\frac{df_n}{dx} \frac{df_p}{dx} - \left(\epsilon_r k_0^2 \right) f_n f_p \right] dx, \qquad \begin{matrix} n = 1, 3, \cdots \\ p = 1, 3, \cdots \end{matrix}. \tag{8}$$

It is assumed that the $\phi_m(x)$ are normalized to unity, i.e., that

$$\int_0^a \phi_m^2 \, dx = \sum_1^N a_n^{(m)^2} \int_0^a f_n^2(x) \, dx = \sum_{n=1}^{N} a_n^{(m)^2} = 1. \tag{9}$$

The equations in (7) form a system of N linear equations in N unknowns and have nonvanishing solutions only for those values of γ_m that make the determinant of the coefficients vanish. Thus, they determine N real values for γ_m^2 and N corresponding eigenvectors $a_n^{(m)}$. The algebraically smallest value of γ_m^2 corresponds to the dominant mode. If only a single mode propagates at the frequency of operation, then γ_1^2 is less than zero, while all other γ_m^2 are positive.

C. Application to a Specific Slab-Loaded Configuration

If the rectangular dielectric slab-loaded guide in Fig. 2 is excited in such a way that only the modes that are symmetrical about $x = a/2$ are excited, then only those modes that correspond to odd index values will be required, and the expressions for T_{np} will be given as follows:

$$T_{np} = T_{pn} = \frac{\sin\left([n-p] \frac{\pi}{2} \right)}{[n-p] \frac{\pi}{2}} \left[np \left(\frac{\pi}{a} \right)^2 - \epsilon_{1r} k_0^2 \right] - k_0^2 [\epsilon_{1r} - \epsilon_{2r}] \left[\frac{\sin\left([n-p] \frac{\pi}{2} \left(1 - \frac{t_1}{a} \right) \right)}{[n-p] \frac{\pi}{2}} - \frac{\sin\left([n+p] \frac{\pi}{2} \left(1 - \frac{t_1}{a} \right) \right)}{[n+p] \frac{\pi}{2}} \right] - k_0^2 [\epsilon_{2r} - 1] \left[\frac{\sin\left([n-p] \frac{\pi}{2} \left(1 - \frac{t_2}{a} \right) \right)}{[n-p] \frac{\pi}{2}} - \frac{\sin\left([n+p] \frac{\pi}{2} \left(1 - \frac{t_2}{a} \right) \right)}{[n+p] \frac{\pi}{2}} \right]. \tag{10}$$

If these expressions are applied to the equations in (7), the propagation constants γ_m and the corresponding eigenvectors $a_n^{(m)}$ can be obtained through the use of standard computer library subroutines. These propagation constants and eigenvectors can then be used in a mode-matching technique to determine the equivalent circuit, as will be described in the following section.

D. Application of Boundary Conditions

In guides 0 and 1, the modes are approximated by the following expressions:

$$\phi_n^{(0)} = \sum_{m=1}^{M} b_m^{(n)} f_m(x) \tag{11a}$$

$$\phi_n^{(1)} = \sum_{m=1}^{M} a_m^{(n)} f_m(x). \tag{11b}$$

The electric-field strengths in the two guides are then given approximately by

$$E_y = A_1 \sin |\Gamma_1| (z + d) \sum_m^M b_m^{(1)} f_m + \sum_{n=3,5,}^{N_1} A_n \left(\sum_m^M b_m^{(n)} f_m \right) e^{\Gamma_n z}, \qquad z < 0 \tag{12a}$$

$$E_y = B_1 \sin |\gamma_1| (z - l) \sum_m^M a_m^{(1)} f_m + \sum_{n=3,5,}^{N_2} B_n \left(\sum_m^M a_m^{(n)} f_m \right) e^{-\gamma_n z}, \qquad z > 0. \tag{12b}$$

In these equations, it is assumed that the short circuit is far enough from the junction that the higher order modes in guide 1 die out before reaching it. The transverse magnetic-field strength is proportional to the z derivative of E_y

$$\frac{\partial E_y}{\partial z} = A_1 |\Gamma_1| \cos |\Gamma_1| (z + d) \sum_m^M b_m^{(1)} f_m + \sum_{n=3,5,}^{N_1} \Gamma_n A_n \left(\sum_m^M b_m^{(n)} f_m \right) e^{\Gamma_n z}, \qquad z < 0 \tag{13a}$$

$$\frac{\partial E_y}{\partial z} = B_1 |\gamma_1| \cos |\gamma_1| (z - l) \sum_m^M a_m^{(1)} f_m - \sum_{n=3,5,}^{N_2} \gamma_n B_n \left(\sum_m^M a_m^{(n)} f_m \right) e^{-\gamma_n z}, \qquad z > 0. \tag{13b}$$

Since the number of terms in the series is finite, the terms in (12) and (13) can be regrouped in the following manner:

$$E_y = \sum_m^M \left(A_1 \sin |\Gamma_1| (z + d) b_m^{(1)} + \sum_{n=3,5,}^{N_1} A_n b_m^{(n)} e^{\Gamma_n z} \right) f_m(x), \qquad z < 0 \tag{14a}$$

$$E_y = \sum_m^M \left(B_1 \sin|\gamma_1|(z-l) a_m^{(1)} + \sum_{n=3,5,}^{N_2} B_n a_m^{(n)} e^{-\gamma_n z} \right) f_m(x), \qquad z>0 \tag{14b}$$

$$\frac{\partial E_y}{\partial y} = \sum_m^M \left(|\Gamma_1| A_1 b_m^{(1)} \cos|\Gamma_1|(z+d) + \sum_{n=3,5,}^{N_1} \Gamma_n A_n b_m^{(n)} e^{\Gamma_n z} \right) f_m(x), \qquad z<0 \tag{14c}$$

$$\frac{\partial E_y}{\partial y} = \sum_m^M \left(|\gamma_1| B_1 a_m^{(1)} \cos|\gamma_1|(z-l) - \sum_{n=3,5,}^{N_2} \gamma_n B_n a_m^{(n)} e^{-\gamma_n z} \right) f_m(x), \qquad z>0. \tag{14d}$$

Given the continuity requirements on the transverse components of E and H at $z=0$, the coefficients of the f_m can be equated for $x=0$ to give the following sets of equations:

$$b_m^{(1)} A_1 \sin|\Gamma_1|d + \sum_{n=3,5,}^{N_1} b_m^{(n)} A_n = -a_m^{(1)} B_1 \sin|\gamma_1|l + \sum_{n=3,5,}^{N_2} B_n a_m^{(n)}, \qquad m=1,2,\cdots,M \tag{15a}$$

$$b_m^{(1)} |\Gamma_1| A_1 \cos|\Gamma_1|d + \sum_{n=3,5,}^{N_1} b_m^{(n)} \Gamma_n A_n = a_m^{(1)} B_1 |\gamma_1| \cos|\gamma_1|l - \sum_{n=3,5,}^{N_2} \gamma_n B_n a_m^{(n)}, \qquad m=1,2,\cdots,M. \tag{15b}$$

When one makes the substitutions

$$A_1' = A_1 \cos|\Gamma_1|d \tag{16a}$$

$$B_1' = B_1 \cos|\gamma_1|l \tag{16b}$$

the set of equations takes the following form:

$$b_m^{(1)} A_1' \tan|\Gamma_1|d + \sum_{n=3,5,}^{N_1} b_m^{(n)} A_n + a_m^{(1)} B_1' \tan|\gamma_1|l - \sum_{n=3,5,}^{N_2} B_n a_m^{(n)} = 0 \tag{17a}$$

$$\times b_m^{(1)} |\Gamma_1| A_1' + \sum_{n=3,5,}^{N_1} b_m^{(n)} \Gamma_n A_n - a_m^{(1)} |\gamma_1| B_1' + \sum_{n=3,5,}^{N_2} \gamma_n B_n a_m^{(n)} = 0. \tag{17b}$$

These equations have $(N_1+N_2+2)/2$ unknowns. If M is made equal to $(N_1+N_2+2)/2$, the system will have as many equations as unknowns. For a nonvanishing solution, the determinant of the coefficients must vanish. The determinant can be expanded in such a way that the requirement that it vanish is put into the form of (1), with

$$A = |\Gamma_1||\gamma_1|\Delta_A \tag{18a}$$

$$B = -|\Gamma_1|\Delta_B \tag{18b}$$

$$C = -|\gamma_1|\Delta_C \tag{18c}$$

$$D = \Delta_D \tag{18d}$$

where the Δ's are defined in Appendix II.

These expressions are easily evaluated on a digital computer. The equations in (2) can then be used to determine the equivalent-circuit parameters.

E. Numerical Results

The foregoing analysis has been applied to several configurations (see Fig. 6(a)–(e)). The specific dimensions and permittivities of these configurations are outlined in Table I, while the equivalent-circuit parameters are shown as a function of t_1/a in Fig. 7(a)–(f).

Configuration A is just the junction of an empty guide and a single centered slab. The thickness of the slab was increased from zero until approximately the point at which the next highest order of symmetric mode propagates. For nonzero slab thicknesses, the apparent electrical length of the unloaded guide increases, while that of the loaded guide decreases. The magnitude of the effect depends on slab thickness. The value of the turns ratio n remains quite close to unity over a large portion of the range, indicating that the principal effect is a phase change of the reflection coefficient. The phase of the transmitted wave is not greatly affected, since the signs of the length changes are opposite and tend to cancel. This form of the equivalent circuit immediately shows that adjusting the lengths of the two guides can compensate for these phase shifts.

Configuration B is a similar junction but with a sandwich structure in one guide. In this configuration, t_2 is fixed and t_1 is increased until approximately the point at which the next symmetric mode propagates. Because of the presence of the second dielectric slab of fixed width, the arrangement is never matched; as in case A, the loaded guide is shortened while the empty guide is lengthened electrically. When t_1 is small—that is, when the slab is mainly a low-permittivity dielectric—the turns ratio is close to unity but rises somewhat for larger values of t_1/a. This rise will affect the magnitude of the reflection and transmission coefficients to some extent, but here again, correcting the physical line lengths may compensate for the phases.

Configuration C shows the junction of two guides, both loaded with the same dielectric material. The thickness t_3 is fixed, while t_1/a is varied until the next higher symmetric mode propagates. When the two slab thicknesses are the same, the junction is matched. For a large range of t_1/a on either side of this value, n is very close to unity and never departs from unity to a significant extent for any t_1/a. In this case, the main effect is a phase shift of the reflection coefficients. The transmission phase is hardly affected, since the θ's are nearly equal and opposite.

Configurations D and E are similar; the only difference between them lies in the thickness t_3 of the high-permittivity dielectric. In these cases, t_1 is varied from zero to t_2, the thickness of the low-permittivity dielectric. Again, the main effect is a small phase shift of the reflection coefficients.

Configuration F shows a variation that differs somewhat from the other configurations. As t_1/a is varied from zero to the point at which the next higher symmetric mode propagates, a matched condition is reached—even though the dielectric slabs are not identical in this case. Rather than approaching zero, the electrical correction terms approach plus or minus $\pi/2$, indicating a large, rapid change of the phase of the reflection coefficients from what theory predicts without the junction equivalent circuit. However, the magnitudes of the reflection coefficients in this region are very small, since the junction is nearly matched. At the matched point, the phase change reaches 180°. The phase of the transmitted wave is unaffected, since the line-length changes are equal and opposite. For widths farther away from the matched condition, the main effect is once again a change in the phase of the reflection coefficients.

Fig. 8 shows the parameters of the equivalent circuit of Fig. 3 for configuration D. While it is evident that a match occurs for large values of X_2, for small values of X_1, and for $Z_1 = 1$, it is not evident from this form of the circuit what the main effects would be away from this condition or how one would compensate for these effects.

III. Conclusion

A method has been presented for the evaluation of equivalent-circuit parameters of junctions of dielectrically loaded rectangular waveguides. This method, which is an extension of the two-mode method of Collin [3]–[6] but differs from that of Chang [1], [2], can be easily programmed for a digital computer. Results have been presented for several junction configurations using the transmission-line form of the equivalent circuit, which readily lends itself to the estimation of the main effects of the junction and to methods for compensating for these effects.

Appendix I
Equivalent-Circuit Parameters in Terms of *ABCD*

In terms of the equivalent-circuit and loading condition shown in Fig. 9, the input impedance at ϕ_1 can be calculated to be

$$Z_{\text{in}} = \frac{jn^2 Z_1 \tan(\theta_2+\phi_2)\cos(\theta_1+\phi_1) + jZ_c \sin(\theta_1+\phi_1)}{Z_c \cos(\theta_1+\phi_1) - n^2 Z_1 \tan(\theta_2+\phi_2)\sin(\theta_1+\phi_1)}. \tag{A1}$$

If ϕ_1 is selected so that Z_{in} is zero, then the following equation must be satisfied:

$$\tan(\phi_1+\theta_1) = -N^2 \tan(\phi_2+\theta_2) \tag{A2}$$

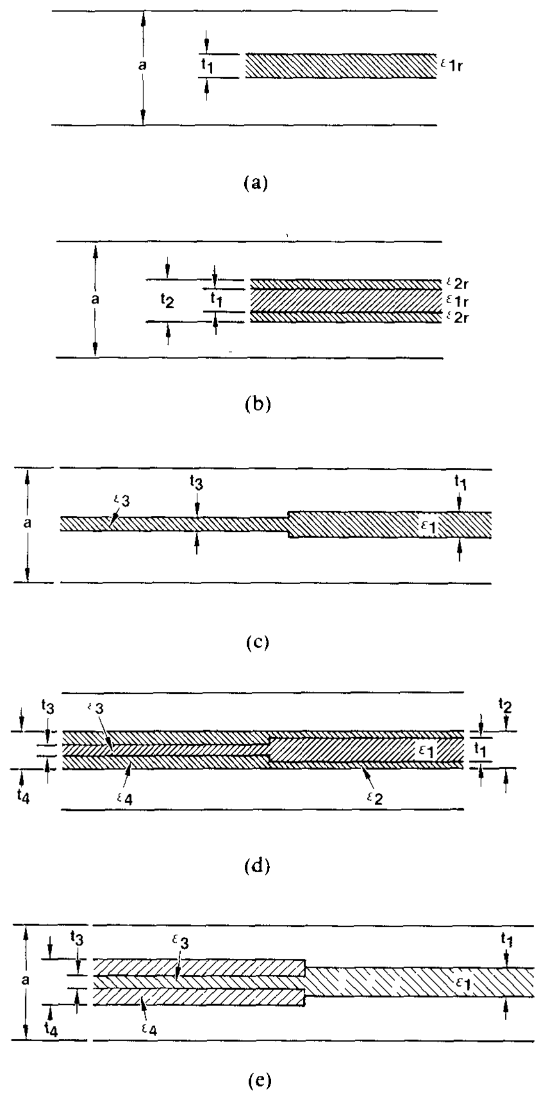

Fig. 6. (a) Junction of empty guide and single-slab-loaded guide (top view, configuration A). (b) Junction of empty guide and composite-slab-loaded guide (top view, configuration B). (c) Junction of slab-loaded guides—same dielectric material on each side (top view, $\epsilon_1 = \epsilon_3$, configuration C). (d) Junction of composite-slab-loaded guides, $\epsilon_1 = \epsilon_3$ and $\epsilon_2 = \epsilon_4$, $t_2 = t_4$ (top view, configurations D and E). (e) Junction of guide with composite slab and guide with single slab (top view, $\epsilon_1 = \epsilon_3$, configuration F).

TABLE I
Dimensions and Relative Permittivities for Cases A through F

VARIABLE	CASE A	B	C	D	E	F
FREQUENCY (GHz)	9 54261	9 54261	9 54261	9.54261	9 54261	9 54261
GUIDE WIDTH (IN)	0 900	0 900	0 900	0 900	0 900	0 900
t_2 (IN)	–	0 495	–	0 315	0.315	–
ϵ_{2r}	–	2.65	–	2.65	2 65	–
t_3 (IN.)	–	–	0 200	0 200	0 100	0 100
ϵ_{3r}	–	–	9 00	9 00	9 00	9 00
t_4 (IN)	–	–	–	0 315	0 315	0 300
ϵ_{4r}	–	–	–	2 65	2 65	2 65
ϵ_{1r}	9 00	9.00	9 00	9 00	9 00	9 00

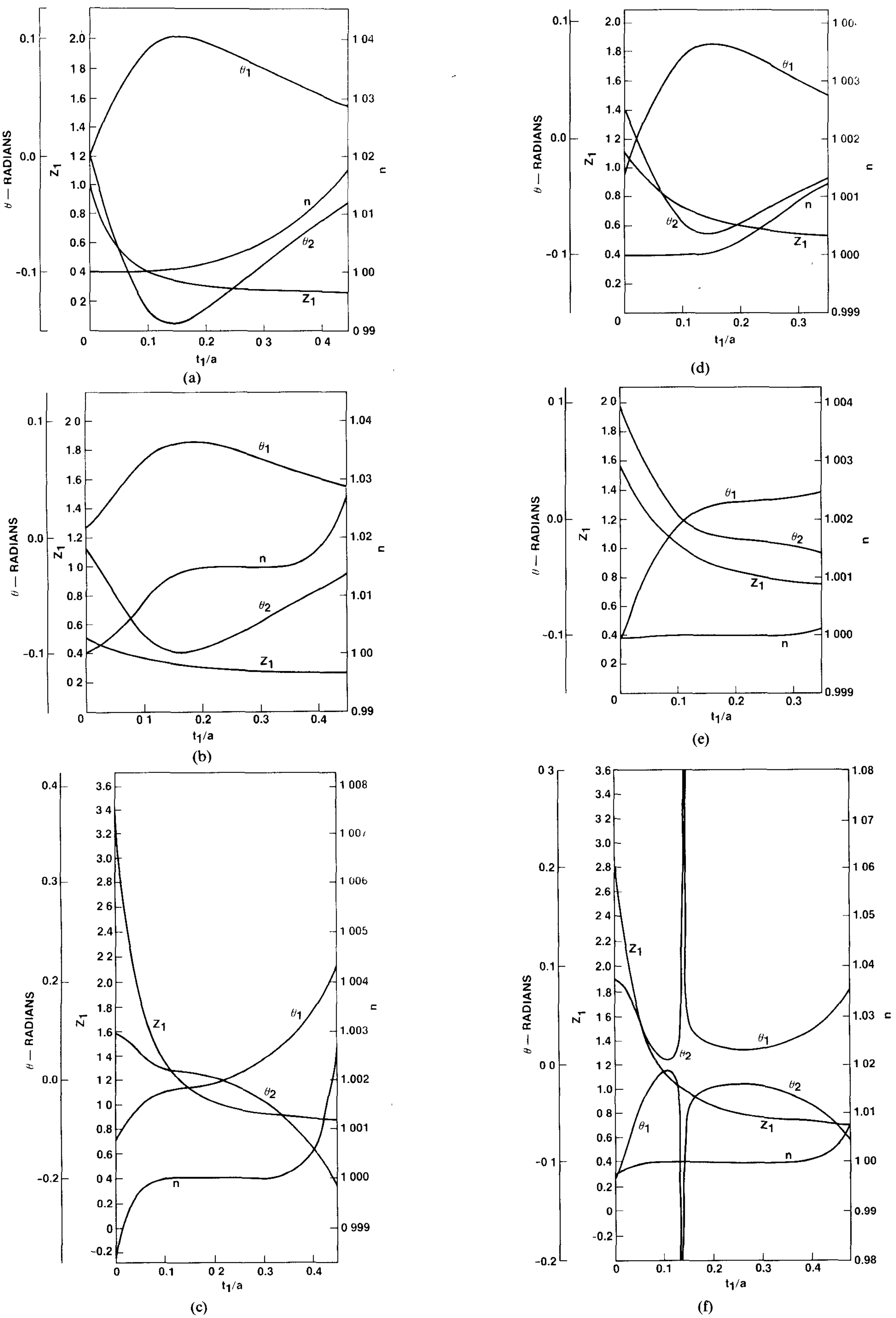

Fig. 7. Equivalent-circuit parameters of configurations A through F.

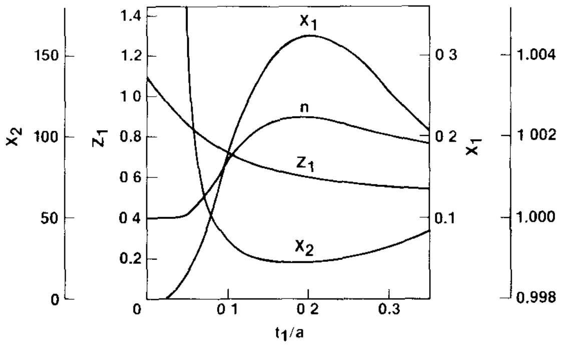

Fig. 8. Parameters of Collin's lumped-element equivalent circuit for configuration D.

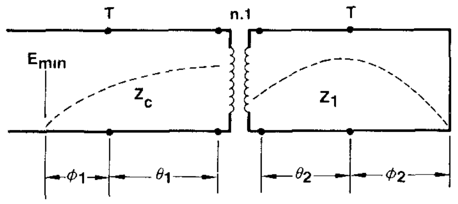

Fig. 9. Arrangement for determining equivalent-circuit parameters.

where

$$N^2 \equiv n^2 \frac{Z_1}{Z_c}. \tag{A3}$$

On using the expression for the tangent of the sum of two angles, (A2) can be written in the following form:

$$\tan\phi_1 = \frac{A + B\tan\phi_2}{C + D\tan\phi_2} \tag{A4}$$

where

$$A = N^2\tan\theta_2 + \tan\theta_1 \tag{A5a}$$

$$B = N^2 - \tan\theta_2\tan\theta_1 \tag{A5b}$$

$$C = N^2\tan\theta_1\tan\theta_2 - 1 \tag{A5c}$$

$$D = N^2\tan\theta_1 + \tan\theta_2 \tag{A5d}$$

From the equations in (A5), we can derive the following expression:

$$\frac{A+D}{B-C} = \frac{\tan\theta_2 + \tan\theta_1}{1 - \tan\theta_1\tan\theta_2} \equiv \tan(\theta_2 + \theta_1). \tag{A6}$$

In a similar manner

$$\frac{A-D}{B+C} = \tan(\theta_2 - \theta_1). \tag{A7}$$

Consequently, the equivalent-circuit parameters are given by the following expressions:

$$\theta_2 = \frac{1}{2}\left[\tan^{-1}\left(\frac{A+D}{B-C}\right) + \tan^{-1}\left(\frac{A-D}{B+C}\right)\right] \tag{A8a}$$

$$\theta_1 = \frac{1}{2}\left[\tan^{-1}\left(\frac{A+D}{B-C}\right) - \tan^{-1}\left(\frac{A-D}{B+C}\right)\right] \tag{A8b}$$

$$N^2 = \frac{\tan\theta_1 - \frac{A}{D}\tan\theta_2}{\frac{A}{D}\tan\theta_1 - \tan\theta_2}. \tag{A8c}$$

Therefore, if we can find quantities proportional to A, B, C, and D, the equivalent-circuit parameters can be determined.

Appendix II
System Determinants

The equations in (17) can be rearranged in such a way that the determinant of the coefficients takes the following form:

$$\Delta = \begin{vmatrix} b_1^{(1)}\tan|\Gamma_1|d & a_1^{(1)}\tan|\gamma_1|l & b_1^{(3)} & -a_1^{(3)} & b_1^{(3)} & -a_1^{(5)} & \cdots & b_1^{(N)} & -a_1^{(N)} \\ b_1^{(1)}|\Gamma_1| & -a_1^{(1)}|\gamma_1| & \Gamma_3 b_1^{(3)} & \gamma_3 a_1^{(3)} & \Gamma_5 b_1^{(5)} & \gamma_5 a_1^{(5)} & \cdots & \Gamma_N b_1^{(N)} & \gamma_N a_1^{(N)} \\ b_3^{(1)}\tan|\Gamma_1|d & a_3^{(1)}\tan|\gamma_1|l & b_3^{(3)} & -a_3^{(3)} & b_3^{(5)} & -a_3^{(5)} & \cdots & b_3^{(N)} & -a_3^{(N)} \\ b_3^{(1)}|\Gamma_1| & -a_3^{(1)}|\gamma_1| & \Gamma_3 b_3^{(3)} & \gamma_3 a_3^{(3)} & \Gamma_5 b_3^{(5)} & \gamma_5 a_3^{(5)} & \cdots & \Gamma_N b_3^{(N)} & \gamma_N a_3^{(N)} \\ b_5^{(1)}\tan|\Gamma_1|d & a_5^{(1)}\tan|\gamma_1|l & b_5^{(3)} & -a_5^{(3)} & b_5^{(5)} & -a_5^{(5)} & \cdots & b_5^{(N)} & -a_5^{(N)} \\ b_5^{(1)}|\Gamma_1| & -a_5^{(1)}|\gamma_1| & \Gamma_3 b_5^{(3)} & \gamma_3 a_5^{(3)} & \Gamma_5 b_5^{(5)} & \gamma_5 a_5^{(5)} & \cdots & \Gamma_N b_5^{(N)} & \gamma_N a_5^{(N)} \\ \vdots & \vdots & \vdots & \vdots & \vdots & \vdots & & \vdots & \vdots \\ b_N^{(1)}\tan|\Gamma_1|d & a_N^{(1)}\tan|\gamma_1|l & b_N^{(3)} & -a_N^{(3)} & b_N^{(5)} & -a_N^{(5)} & \cdots & b_N^{(N)} & -a_N^{(N)} \\ b_N^{(1)}|\Gamma_1| & -a_N^{(1)}|\gamma_1| & \Gamma_3 b_N^{(3)} & \gamma_3 a_N^{(3)} & \Gamma_5 b_N^{(5)} & \gamma_5 a_N^{(5)} & \cdots & \Gamma_N b_N^{(N)} & \gamma_N a_N^{(N)} \end{vmatrix} \tag{A9}$$

The determinant Δ_A in the equations in (18) is given by the following expression:

$$\Delta_A = \begin{vmatrix} 0 & 0 & b_1^{(3)} & -a_1^{(3)} & b_1^{(5)} & -a_1^{(5)} & \cdots & b_1^{(N)} & -a_1^{(N)} \\ a_1^{(1)} & b_1^{(1)} & \Gamma_3 b_1^{(3)} & \gamma_3 a_1^{(3)} & \Gamma_5 b_1^{(5)} & \gamma_5 a_1^{(5)} & \cdots & \Gamma_N b_1^{(N)} & \gamma_N a_1^{(N)} \\ 0 & 0 & b_3^{(3)} & -a_3^{(3)} & b_3^{(5)} & -a_3^{(5)} & \cdots & b_3^{(N)} & -a_3^{(N)} \\ a_3^{(1)} & b_3^{(1)} & \Gamma_3 b_3^{(3)} & \gamma_3 a_3^{(3)} & \Gamma_5 b_3^{(5)} & \gamma_5 a_3^{(5)} & \cdots & \Gamma_N b_3^{(N)} & \gamma_N a_3^{(N)} \\ 0 & 0 & b_5^{(3)} & -a_5^{(3)} & b_5^{(5)} & -a_5^{(5)} & \cdots & b_5^{(N)} & -a_5^{(N)} \\ a_5^{(1)} & b_5^{(1)} & \Gamma_3 b_5^{(3)} & \gamma_3 a_5^{(3)} & \Gamma_5 b_5^{(5)} & \gamma_5 a_5^{(5)} & \cdots & \Gamma_N b_5^{(N)} & \gamma_N a_5^{(N)} \\ \vdots & \vdots & \vdots & \vdots & \vdots & \vdots & & \vdots & \vdots \\ 0 & 0 & b_N^{(3)} & -a_N^{(3)} & b_N^{(5)} & -a_N^{(5)} & \cdots & b_N^{(N)} & -a_N^{(N)} \\ a_N^{(1)} & b_N^{(1)} & \Gamma_3 b_N^{(3)} & \gamma_3 a_N^{(3)} & \Gamma_5 b_N^{(5)} & \gamma_5 a_N^{(5)} & \cdots & \Gamma_N b_N^{(N)} & \gamma_N a_N^{(N)} \end{vmatrix} \tag{A10}$$

Δ_B is the same as Δ_A except that the first column is replaced by $a_1^{(1)}, 0, a_3^{(1)}, 0, a_5^{(1)}, 0, \cdots, a_N^{(1)}, 0$. Δ_C is the same as Δ_A except that the second column is replaced by $b_1^{(1)}, 0, b_3^{(1)}, 0, \cdots, b_N^{(1)}, 0$. Δ_D is the same as Δ_C with the first column replaced by $a_1^{(1)}, 0, a_3^{(1)}, 0, a_5^{(1)}, 0, \cdots, a_N^{(1)}, 0$.

Acknowledgment

The author would like to thank C. Williams and A. Fellows for their efforts in the editing of this manuscript.

References

[1] C. T. M. Chang, "Equivalent circuit for partially dielectric-filled rectangular waveguide junctions," *IEEE Trans. Microwave Theory Tech.*, vol. MTT-21, pp. 403–411, June 1973.

[2] C. T. M. Chang, "Partially dielectric-slab-filled waveguide phase shifter," *IEEE Trans. Microwave Theory Tech.*, vol. MTT-22, pp. 481–485, May 1974.

[3] R. E. Collins, *Field Theory of Guided Waves*. New York: McGraw-Hill, 1960, pp. 237–247.

[4] R. E. Collin, "Properties of dielectric slotted interfaces," *IRE Trans. Ant. Propagat.*, vol. AP-7, pp. 62–73, Jan. 1959.

[5] R. E. Collin, "Reflection and transmission at a slotted dielectric interface," *Can. J. Phys.*, vol. 34, pp. 398–411, Apr. 1956.

[6] R. E. Collin, "Determination of equivalent circuit parameters," *IRE Trans. Microwave Theory Tech.*, vol. MTT-5, pp. 266–267, Oct. 1957.

Alfred T. Villeneuve (S'52–A'53–M'58–SM'82) was born in Syracuse, NY. He received the B.E.E. degree from Manhattan College, Bronx, NY, in 1952, and the M.E.E. and Ph.D. degrees from Syracuse University, Syracuse, NY, in 1955 and 1959, respectively.

From 1952 to 1955, he was a Research Associate in Electrical Engineering at Syracuse University, where he worked on UHF antennas and microwave filters. From 1956 to 1959, he was an Instructor in Electrical Engineering, teaching courses in electromagnetism and network theory. In 1959, he was promoted to Assistant Professor. In the same year, he joined Hughes Aircraft Co., where he is currently a Chief Scientist in the Antenna Systems Laboratory of the Radar Systems Group. He has been engaged in various aspects of antenna theory and design there over the past 26 years. He has been a lecturer at the University of Southern California, the University of California at Los Angeles, and at Loyola-Marymount University in Los Angeles.

Dr. Villeneuve has served as a reviewer for the IEEE TRANSACTIONS ON MICROWAVE THEORY AND TECHNIQUES AND IEEE TRANSACTIONS ON ANTENNAS AND PROPAGATION and has served a term on the Administrative Committee of the Antennas and Propagation Society (AP-S). He also served as Secretary-Treasurer, Vice Chairman, and Chairman of the Los Angeles Chapter of AP-S. He is a member of the IEEE Antenna Standards Committee and was a member of Subcommittee 2.11 on Methods of Testing Antennas which recently published IEEE Std 149-1979, *IEEE Standard Test Procedures for Antennas*. He was a member of the Working Group on Definition of Terms for Antennas which recently completed IEEE Std 145-1983, *IEEE Standard Definitions of Terms for Antennas*. He served on the Steering Committees of the 1971 and 1981 International Antennas and Propagation Symposia and has also been on the Technical Program committees of these and several other symposia. He is a member of Eta Kappa Nu, Sigma Xi, and Commission B of the International Union of Radio Science.